Two-pulse laser control for selective photofragment orientation

Machholm, Mette; Henriksen, Niels Engholm

Published in:
Journal of Chemical Physics

Link to article, DOI:
10.1063/1.479585

Publication date:
1999

Document Version
Publisher's PDF, also known as Version of record

Two-pulse laser control for selective photofragment orientation

Mette Machholm[a)]
Department of Chemistry, Aarhus University, Langelandsgade 140, DK-8000 Aarhus C, Denmark

Niels E. Henriksen[b)]
Department of Chemistry, Technical University of Denmark, DTU 207, DK-2800 Lyngby, Denmark

(Received 3 March 1999; accepted 24 May 1999)

The nuclear wave packet dynamics in the potential well of a bound molecule can be controlled by an intense infrared (IR)-laser pulse. The phase of the nuclear wave packet motion is shown to depend on the phase of the laser field and the initial orientation of the molecule. We demonstrate, for diatomic heteronuclear molecules, that these spatial effects can be used to control the angular distribution of photofragments by selective dissociation of molecules with a given initial orientation from a sample of randomly oriented molecules. © *1999 American Institute of Physics.* [S0021-9606(99)01131-9]

I. INTRODUCTION

Active control of unimolecular reactions, e.g., selective bond breaking of polyatomic molecules, is a major challenge in modern photochemistry.[1] Many of the proposed schemes are variants of pump–probe schemes,[2] where wave packet (WP) dynamics is initiated by a pump laser pulse and subsequently probed by a second pulse. The timing of the pump and control pulses determines the outcome of the photoreaction. Instead of being only an initiator, the pump pulse can actively control the dynamics of the WP by forcing the motion of the WP. Then, the combined laser field and molecular potential determines the WP evolution. We consider a two-step control scheme of the latter kind which consists of (i) preparation of a nonstationary vibrational WP with an intense infrared (IR) laser pulse, and subsequently (ii) bond breaking, where a part of the WP is transferred to a new dissociative electronic state by a short-pulse ultraviolet (UV) laser pulse. The control scheme has been used in theoretical studies of selective bond breaking of triatomic molecules.[3–5]

The WP dynamics of a molecule in a bound state can be driven by an IR-laser field if the molecule possesses a dipole moment with a nonzero derivative.[6] In the harmonic limit, an IR-laser field in resonance with the $v=0\rightarrow v=1$ transition ($\omega_{\mathrm{IR}}=\omega_0$) will force the WP to oscillate with the frequency of the field ω_{IR}. The amplitude of the oscillations will be proportional to the pulse area (electric field amplitude times pulse length). The width of the WP stays constant independent of the amplitude of the oscillations; thus, the motion resembles classical motion. In the case of nearly harmonic potentials, the spread of the WP will be small, and only for large amplitude oscillations or after many oscillations will the spread of the WP be large compared to the initial width.

The analytical model and the simulations to be presented in this paper show that the dynamics of the nonstationary vibrational WP is sensitive to the phase of the laser field and the initial orientation of the molecule. These spatial effects imply some complications for the control scheme for selective bond breaking,[3–5] but also provide new possibilities for controlling the spatial distribution of photofragments, which is the main subject of the present paper. The orientational dependence of the IR-laser excitation is such that molecules oppositely oriented in space will oscillate phase shifted by π. We use this spatial effect in a control scheme that enables spatial separation of different photofragments. The control scheme is sketched in Fig. 1 for a heteronuclear diatomic *AB* molecule: (i) an intense IR-laser pulse is applied on molecules initially in the electronic ground-state potential well, thereby forcing the nearly harmonic oscillator, (ii) depending on the frequency of a second laser pulse, molecules at a given internuclear separation R_{control} can be excited resonantly to a repulsive state, thereby selectively dissociating the molecules at R_{control}. If the second laser pulse is shorter than the optical cycle of the first laser pulse, only some of the oscillating molecules will pass R_{control} during the second pulse. Now, taking into account that molecules oriented initially as *AB* or *BA* will oscillate out of phase, *AB* being at the inner turning point when *BA* reaches the outer turning point, then if R_{control} is at the outer turning point, only *BA* or *AB* molecules will be dissociated depending on the timing of the control pulse relative to the IR-pump pulse. The control scheme is demonstrated by application to selective dissociation of one particular orientation of NaI molecules in a sample of randomly oriented molecules.

In the present scheme, the angular distribution of photofragments is controlled via the timing of two laser pulses. Alternatively, quantum mechanical interference controlled by the relative phase of two laser fields has been used to achieve directional control. With two intense pulses, isotope separation of HD^+ has been demonstrated.[7] Recently, a scheme in the weak field limit, where the dissociation probability depends on the relative phase has been proposed.[8]

The present paper is organized as follows: The model for the numerical simulations is given in Sec. II A. Section II B summarizes the corresponding analytical result for a har-

[a)]Present address: 23 Holland Hill, #B1-11 Holland Peak, Singapore 278739.
[b)]Electronic mail: neh@kemi.dtu.dk

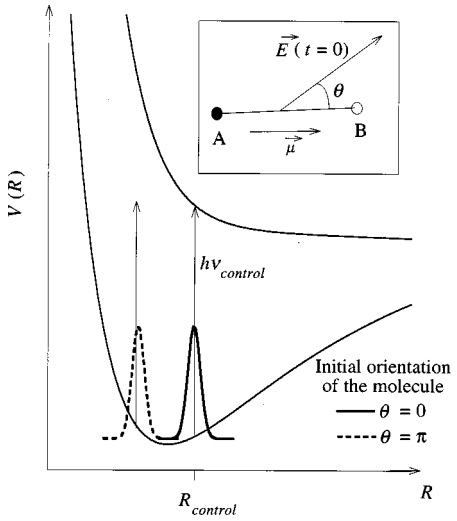

FIG. 1. Control scheme for selective dissociation of heteronuclear diatomic molecules *AB*, initially oriented with either the *A* or the *B* atom towards the detector, given by the angle θ between the permanent dipole moment $\vec{\mu}$ and the electric field vector $\vec{E}$. At $t=t_{\text{control}}$, oppositely oriented molecules driven by the IR field will have the bond stretched (e.g., $\theta=0$) or shortened (e.g., $\theta=\pi$).

monic potential. The second step in the control scheme is described in Sec. II C. The results for spatial separation of Na and I in dissociation of NaI are presented in Sec. III. In the conclusion, we comment on the implications of the orientational effect for the selective bond-breaking control scheme by Amstrup and Henriksen.[3,4]

II. HETERONUCLEAR DIATOMIC MOLECULE DRIVEN BY AN INTENSE IR-LASER PULSE

A. Numerical simulations: One- and three-dimensional models

We consider a 1D- and a 3D- model of a heteronuclear diatomic molecule in the electronic ground state. The molecule is driven by an intense IR-laser pulse. In the 3D model, the wave function is expanded in spherical harmonics. The laser light is linearly polarized, giving the selection rule $\Delta m=0$, when the laser polarization vector and the quantization axis are parallel. Thus, m is conserved and each initial m can be treated individually

$$\Psi_m(\mathbf{R},t)=\sum_l \chi_l(R,t)Y_{lm}(\theta,\phi), \tag{1}$$

$m=0$ in the following unless explicitly given. The Hamiltonian consists of a field-free molecular term and an interaction IR term

$$\hat{H}(R,t)=\hat{H}_{\text{mol}}(R)+\hat{H}_{\text{IR}}(R,t). \tag{2}$$

The first step in the control scheme involves only the electronic ground state. In Sec. II C, the coupling to the first excited state involved in the control step will be included. In the 1D model, the IR-interaction term is

$$\hat{H}_{\text{IR}}(R,t)=\pm\mu_g(R)E(t)\cos(\omega_{\text{IR}}t), \tag{3}$$

where μ_g is the permanent dipole in the ground state. The sign depends on the orientation of the molecule: the minus sign describes the situation where the field and the dipole moment vector are pointing in the same direction ($\theta=0$), whereas the plus sign describes the situation where they have opposite directions ($\theta=\pi$). The orientation-dependent response can be simulated in the 1D model by two 1D calculations with opposite sign in the interaction term, Eq. (3).

In several studies of photodissociation with intense IR pulses, it has been shown that chirping of the laser field can enhance the vibrational excitation (see, e.g., Ref. 9). However, we have investigated the effect of chirp, and found that it is small and often not helpful in the present case characterized by short laser pulses (<1 ps), moderate number of vibrational levels populated, and coherent motion of the WP. Thus, we use a Fourier transform limited Gaussian pulse shape.

In the 3D-model, each l basis state is coupled to $l\pm1$

$$\hat{H}_{\text{IR}}(R,t)=H_{\text{IR}}(R,t)\begin{pmatrix} 0 & V_0^1 & 0 & & 0 & \\ V_0^1 & 0 & V_1^2 & \cdots & 0 & \\ 0 & V_1^2 & 0 & & 0 & \\ & \vdots & & \ddots & V_l^{l+1} & \\ 0 & 0 & 0 & V_l^{l+1} & 0 & \\ & & & & & \ddots \end{pmatrix}, \tag{4}$$

where

$$V_l^{l+1}=\sqrt{\frac{(l+m+1)(l-m+1)}{(2l+3)(2l+1)}},$$
$$H_{\text{IR}}(R,t)=\mu_g(R)E(t)\cos(\omega_{\text{IR}}t). \tag{5}$$

The potential energy term in $\hat{H}_{\text{mol}}(R)$ is a diagonal matrix with the elements

$$V^l_{\text{mol},g}(R)=V_g(R)+\frac{\hbar^2}{2M}\frac{l(l+1)}{R^2}, \tag{6}$$

where M is the reduced mass.

The time-dependent Schrödinger equation is propagated with a split-operator method, where the kinetic energy operator is evaluated via a fast Fourier transform (FFT). The potential energy term and the interaction term of the short-time propagator are split further to avoid numerical diagonalization at each time-step and R-grid point[10]

$$\exp\left(-i(\hat{V}_{\text{mol}}+\hat{H}_{\text{IR}})\frac{dt}{\hbar}\right)$$
$$=\exp\left(-i\hat{V}_{\text{mol}}\frac{dt}{2\hbar}\right)U^{\dagger}\exp\left(-i\hat{H}_{\text{IR}}\frac{dt}{\hbar}\right)U$$
$$\times\exp\left(-i\hat{V}_{\text{mol}}\frac{dt}{2\hbar}\right), \tag{7}$$

where U is a unitary transformation matrix that diagonalizes $\hat{H}_{\text{IR}}$. U is determined numerically only once, because the matrix in Eq. (4) is the same at all time steps and R-grid points.

We follow the WP dynamics by calculating the expectation value of R, $\langle R\rangle$, and the standard deviation: $\Delta R = \sqrt{\langle R^2\rangle - \langle R\rangle^2}$ as a function of time. In the 3D model, $\langle R\rangle$ and ΔR are calculated for $\theta = 0$ and π, where θ is the angle between the internuclear axis and the polarization vector of the field. We also consider the normalized value: $\langle R\rangle_{\text{norm}} = (\langle R\rangle - R_e)/\Delta R$, which gives the displacement of the WP relative to the equilibrium position in units of the width of the wave packet.

B. Analytical model for a harmonic potential

A harmonic potential is a good approximation for the molecular ground-state potential around the equilibrium position. In the harmonic limit and in one dimension, the WP dynamics can be found analytically (see the Appendix). For a resonant IR-field [$\omega_{\text{IR}} = \omega_0$ in Eq. (3)], we have

$$\langle R - R_e\rangle \propto \pm \frac{\mu_g'(R_e) E_{\max} T_{\text{FWHM}}}{\omega_0 M} \sin(\omega_0 t), \tag{8}$$

where $\mu_g'(R_e)$ is the derivative of the dipole moment at the equilibrium bond length, R_e. The amplitude of the oscillation is proportional to the pulse area $E_{\max} T_{\text{FWHM}}$, where T_{FWHM} is the full width half maximum of the intensity pulse shape $I(t) \propto E(t)^2$. From Eq. (8), we observe that the phase of the oscillations depends on the initial orientation of the permanent dipole moment of the molecule. The control scheme proposed in this work uses this orientation dependence.

C. Selective dissociation of molecules with a given orientation

Orientation-dependent WP oscillations induced by the IR pulse allow us to control the spatial photofragment distribution in a subsequent dissociation via an excited state. A delayed short UV-laser pulse excites the molecules having a bond length around R_{control} to a dissociative electronic state. The WP is propagated on the coupled ground and excited states. In 1D, the Hamiltonian is

$$\hat{H}(R,t) = \begin{pmatrix} H_g(R) + H_{\text{IR},g}(R,t) & H_{\text{UV}}(R,t) \\ H_{\text{UV}}(R,t) & H_e(R) + H_{\text{IR},e}(R,t) \end{pmatrix}. \tag{9}$$

The excited electronic state has an IR-interaction term similar to Eq. (3). H_{UV} is similar to Eq. (3) with the permanent dipole moment replaced by the transition dipole moment for the $g \rightarrow e$ transition and with the frequency and pulse shape of the UV-laser field. In 3D, the Hamiltonian is

$$\hat{H}(R,t) = \begin{pmatrix} \hat{H}_{\text{mol},g}(R) + \hat{H}_{\text{IR},g}(R,t) & \hat{H}_{\text{UV}}(R,t) \\ \hat{H}_{\text{UV}}(R,t) & \hat{H}_{\text{mol},e}(R) + \hat{H}_{\text{IR},e}(R,t) \end{pmatrix}, \tag{10}$$

where $\hat{H}_{\text{IR},g}$ and $\hat{H}_{\text{IR},e}$ are given by Eq. (4) with the permanent dipole moment of the relevant state. $\hat{H}_{\text{UV}}$ is similar, with the transition dipole moment instead of μ_g. The potential energy terms in $\hat{H}_{\text{mol},g}$ and $\hat{H}_{\text{mol},e}$ have only diagonal elements, given in the form of Eq. (6).

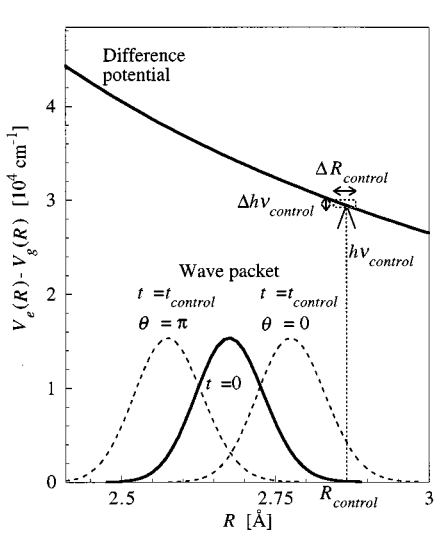

FIG. 2. Difference potential between the ground and first excited-state electronic potentials of NaI. The WP in the electronic ground state is forced to oscillate with an amplitude about the width of the WP. The dashed curve shows the WP at the outer turning point, and the dotted quadrangle indicates the spectral width of a 20 fs pulse and the corresponding excitation region for the control step.

We calculate probabilities for excitation to the excited state as a function of time delay between the pulses and investigate the dependence on the initial orientation.

III. APPLICATION TO NaI

The spacing of the ground-state vibrational levels of NaI is $\hbar\omega_0 \approx 280\ \text{cm}^{-1}$, giving a vibrational period of 119 fs. The potentials are taken from Ref. 11. The R-dependence of the difference potential between the ground and the first excited electronic state of NaI is shown in Fig. 2. The excited state is a predissociating state. Due to the spectral width of the short control pulse, the excitation region is spread out around R_{control} depending on the slope of the difference potential. The spectral width of a 20 fs Fourier transform limited Gaussian pulse ($\hbar\Delta\omega \approx 735\ \text{cm}^{-1}$) and the corresponding excitation region are sketched in the figure. To obtain good selectivity, we choose $R_{\text{control}} > R_e + 1.5\Delta R$; thus, a UV control pulse with wave length >315 nm is needed.

In the 1D model, we consider the orientation of NaI corresponding to $\theta = 0$ as well as $\theta = \pi$. In the full 3D description, we assume, unless the rotational quantum number is explicitly specified in the following, that initially NaI is in the rotational ground state ($l = 0$) corresponding to a (coherent) superposition of randomly oriented molecules. The numerical simulations are fully converged when the rotational levels $l \leqslant l_{\text{initial}} + 20$ are included. For $l_{\text{initial}} = 0$, the $l = 0$ and $l = 1$ levels have the main population at the end of the IR pulse. For $l_{\text{initial}} > 0$, the population of $l = l_{\text{initial}} \pm 1$ are equally important.

A. Ground-state wave packet dynamics

In Fig. 3, we show that a well-localized oscillating WP can easily be created, e.g., a 714 fs-long resonant IR-laser pulse with $I_{\max} = 5 \times 10^9\ \text{W/cm}^2$ can drive oscillations of the WP with an amplitude ≈ 3 times the standard deviation of

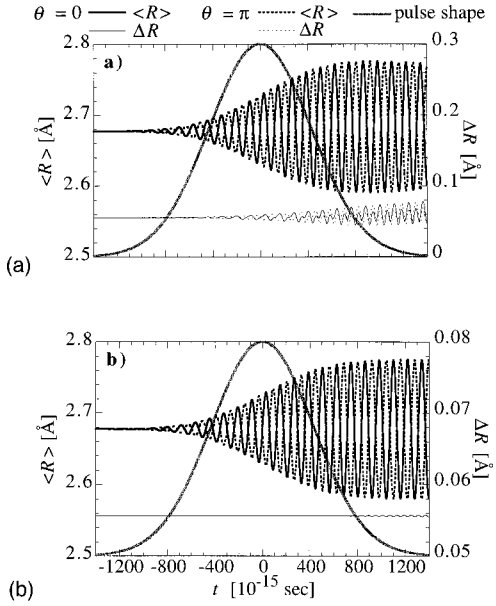

FIG. 3. The expectation value of the bond length as a function of time depending on the initial orientation of the molecule. The phase of the oscillations depends on the direction of the permanent dipole moment. $\hbar\omega = 280\ \mathrm{cm}^{-1}$, $I_{\mathrm{IR}} = 5\times 10^{9}\ \mathrm{W/cm}^2$, FWHM: 6 optical cycles$=714$ fs. The pulse shape plotted is that of the *E*-field. 3D calculations. (a) NaI potential, (b) harmonic potential with similar parameters.

the position. $\langle R\rangle$ oscillates with the frequency of the laser field. The spread of the WP is small, and $\langle R\rangle_{\mathrm{norm}}$ and $\langle R\rangle$ are proportional except for the highest laser intensities studied (result not shown). When the amplitude of the WP oscillations is not too large ($<5\Delta R$), it is proportional to $I_{\mathrm{max}}^{1/2}$ and to E_{max} (the electromagnetic field amplitude at the peak of the IR-laser pulse). For larger amplitude of the oscillations, the anharmonicity of the molecular potential becomes important, and thus the maximum amplitude increases more slowly than $I_{\mathrm{max}}^{1/2}$ for large laser intensities.

The analytical model for the interaction with the IR pulse predicted an orientation-dependent phase of the WP oscillations. This effect is indeed seen in the numerical results. The molecules aligned with the laser polarization vector but with opposite orientation reach the minimum and maximum bond length at the same time. The bond length $\langle R\rangle$ at $\theta=0$ and $\theta=\pi$ is shown in Fig. 3(a). Also, the WP illustrates this result (Fig. 4). The WP obtained in a 3D calculation is plotted as a function of R and θ. The WP is plotted at a time where the opposite-oriented molecules reach the minimum and maximum bond length. Molecules oriented perpendicular to the polarization vector stay vibrationally unexcited.

We have also performed numerical simulation with a harmonic potential adjusted to the parameters of the NaI potential. These results compare very well to the previous ones. The main difference is that the oscillations in the harmonic potential are symmetric around R_e, whereas in the slightly anharmonic potential the molecular bond is stretched about 10% more than it is compressed. The width of the WP stays constant in the 3D harmonic potential calculation, apparently only limited by the numerical precision [notice the factor 10 difference for the *y*-axis scales in Fig. 3(b)]. This finding is in agreement with the prediction of the 1D analytical model. We have compared the full 3D results to the 1D results at $\theta=0$ and $\theta=\pi$. The bond length and WP width are in perfect agreement. In Fig. 3, the 3D results are shown, but similar 1D results cannot be distinguished. The good agreement between the 1D- and the 3D-calculations allows us to model the full three-dimensional WP dynamics with a set of 1D calculations where the orientation of the molecular axis with respect to the field polarization vector is incorporated in the IR-interaction term.

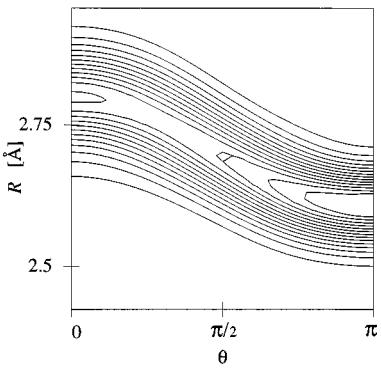

FIG. 4. The wave packet as a function of R and molecular axis orientation in the 3D calculation of Fig. 3(a), $t=990$ fs.

Finally, we consider the effect of rotation. The above results are obtained with the rotational ground state as the initial state. In an experiment, a molecular beam produced by supersonic expansion will be rotationally cold, but with a finite rotational temperature, typically $T<10\,\mathrm{K}$. At 5 K, the $l=3$ and at 10 K the $l=5$ state is the most populated level, and more than 90% of the population is in $l\leqslant 7$ and $l\leqslant 10$, respectively. We have performed calculations with $l=3$, $l=5$, and $l=10$ as initial states. In Fig. 5, we show $\langle R-R_e\rangle_l$ as a function of angle θ at a maximum of $\langle R\rangle$. For initial $l=0$, the data shown are obtained directly from one 3D calculation. For initial $l>0$, several *m*-states contribute, and the curve is a weighted sum of all the *m*-states

$$\langle R-R_e\rangle_l(\theta,t)=\frac{\Sigma_m\langle R-R_e\rangle_{lm}(\theta,t)\,\mathrm{norm}_{lm}(\theta,t)}{\Sigma_m\,\mathrm{norm}_{lm}(\theta,t)}, \quad (11)$$

where l indicates the initial l-state and

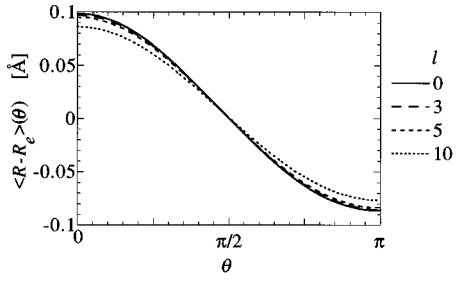

FIG. 5. The dependence on initial rotational level. $\langle R-R_e\rangle_l(\theta,t=990\ \mathrm{fs})$ for different initial l. Laser parameters as in Fig. 3.

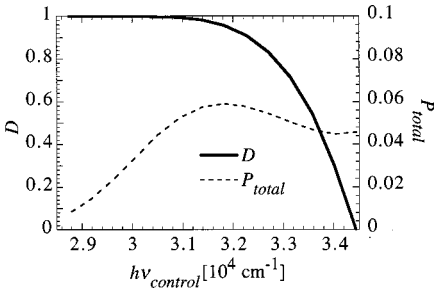

FIG. 6. Frequency dependence of the selectivity parameter D and the total excitation probability $P(\theta=0)+P(\theta=\pi)$ for transition to the excited state. 1D calculation. $T_{\mathrm{peak,UV}}=1015$ fs, $I_{\mathrm{UV}}=10^{12}$ W/cm^2, and $T_{\mathrm{FWHM,UV}}=17$ fs.

$$\mathrm{norm}_{lm}(\theta,t)=\int_{R_{\min}}^{R_{\max}}\Psi_m^*(R,\theta,t)\Psi_m(R,\theta,t)dR. \qquad (12)$$

Figure 5 shows that the response to the IR field is very similar for all initial l considered. The curves for $l=0$ and $l=3$ nearly coincide, and only for $l=10$ is the amplitude of the WP oscillations smaller ($\approx$10%). Therefore, we conclude that for $T<10$ K the rotation: (i) does not decrease the amplitude of the driven oscillations, (ii) does not change the angular dependence of the IR response, and (iii) will not affect the spatial control demonstrated in the next section. Even the width of the fragment distribution should not be changed, because the rotational period ($\approx$100 ps) is much longer than the duration of the control experiment ($\approx$1 ps).

B. Controlling the spatial distribution of photofragments

We now include the control pulse. We calculate the probability for excitation to the dissociative state as a function of the angle θ between the laser field polarization vector and the molecular axis, $P(\theta)$. In the 1D calculations, only $P(\theta=0)$ and $P(\theta=\pi)$ is determined. The selectivity of the photofragment orientation is quantified by

$$D=\frac{P(\theta=0)-P(\theta=\pi)}{P(\theta=0)+P(\theta=\pi)}, \qquad (13)$$

which is in the range from -1 [when $P(\theta=0)=0$] to 1 [when $P(\theta=\pi)=0$]. We also consider the total dissociation probability, in the 1D case given by $P(\theta=0)+P(\theta=\pi)$.

We first consider the dependence on the frequency of the UV control pulse (Fig. 6). For a short control pulse ($T_{\mathrm{FWHM,UV}}\approx 17$ fs) centered around a maximum of $\langle R\rangle$ for $\theta=0$, we see a clear increase in the selectivity as R_{control} is varied from 2.67 Å ($\hbar\omega_{\mathrm{UV}}=34\,400$ cm^{-1}) to 2.89 Å ($\hbar\omega_{\mathrm{UV}}=28\,800$ cm^{-1}). The total dissociation probability decreases for the same variation of R_{control}; thus, the optimum choice of ω_{UV} is a compromise between high selectivity and the number of photofragments. Also, the amplitude of the WP oscillations in the ground-state potential well is important for the selectivity. We find that a very high selectivity ($D>0.996$) can be obtained for reasonable parameters of the IR and UV fields: $I_{\mathrm{IR}}=5\times10^9$ W/cm^2, $T_{\mathrm{FWHM,IR}}=714$ fs, $I_{\mathrm{UV}}=10^{12}$ W/cm^2, $T_{\mathrm{FWHM,UV}}=17$ fs, and $\hbar\omega_{\mathrm{UV}}=30\,500$ cm^{-1}. The total excitation probability is then $P(\theta=0)+P(\theta=\pi)=0.044$.

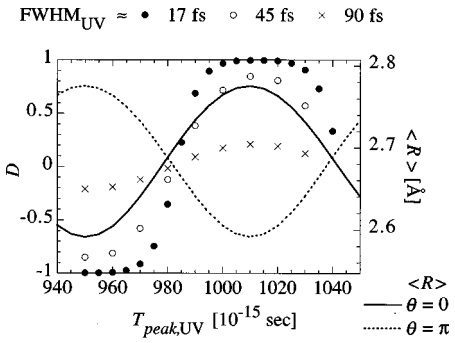

FIG. 7. Delay time $T_{\mathrm{peak,UV}}$ dependence of D compared to the bond length $\langle R\rangle$ of the ground-state molecules. 1D calculation. $\omega_{\mathrm{UV}}=30\,507$ cm^{-1} and $I_{\mathrm{UV}}=10^{12}$ W/cm^2.

The timing and the length of the UV control pulse with respect to the oscillation of the IR field is important for the selectivity (Fig. 7). By changing the timing of the control pulse, we can alter the direction of the Na and I photofragments. When the control pulse length is increased, the selectivity D decreases. When the pulse length becomes larger than the IR field period, the selectivity disappears.

The orientation-dependent excitation probability obtained in a 3D calculation is shown in Fig. 8. The angular dependence of the fragment distribution $P(\theta)$ is obtained by integrating the excited state WP over R. The normalization of the ground-state WP is taken into account. We see that the fragment distribution is very narrow around $\theta=0$. Thus, Na fragments show up only in the forward hemisphere, and I fragments only in the backward hemisphere. Without the IR field, the distribution should be proportional to $\cos^2\theta$. When the excitation is not saturated ($I<10^{13}$ W/cm^2), the fragment distribution around $\theta=0$ is proportional to $|\cos^4\theta|$. When decreasing I, the angular distribution becomes slightly more narrow, but never better than $\propto|\cos^5\theta|$. The total excitation probability stays small in the 3D calculations. With the laser parameters of Fig. 8, the total excitation probability is 0.0043. By increasing I_{UV} to 5×10^{12} W/cm^2, we get 0.0167 without destroying the selectivity or the angular distribution.

Finally, we compare the selectivity (D) found in the 1D and 3D calculations. They agree well, with a slightly better selectivity in the 3D calculations. For example, we find in 1D: $D=0.9961$ and in 3D: $D=0.9983$ with the laser parameters as in Fig. 8. In the 3D calculation, we can take into

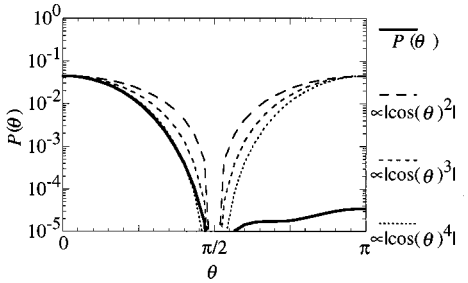

FIG. 8. Angular dependence of the probability for transition to the excited state, $P(\theta)$ for $\omega_{\mathrm{UV}}=30\,507$ cm^{-1}, $T_{\mathrm{peak,UV}}=1015$ fs, $T_{\mathrm{FWHM,UV}}=17$ fs, $I_{\mathrm{IR}}=5\times10^9$ W/cm^2, and $I_{\mathrm{UV}}=10^{12}$ W/cm^2. 3D calculation.

account all fragments in the two hemispheres, such that $P(\theta=0)$ and $P(\theta=\pi)$ in Eq. (13) are replaced by the total dissociation probabilities into the forward and backward hemispheres, respectively. Then, the selectivity decreases to $D_{\text{integral}}=0.9969$, still above the value found in 1D.

IV. CONCLUSION

We have studied vibrational wave packet dynamics driven by an intense infrared laser pulse in heteronuclear diatomic molecules. The analytical model and the numerical results presented in this paper show that the dynamics of the vibrational wave packet depends on the phase of the laser field as well as the initial orientation of the molecule.

We have suggested a new two-pulse scheme for the control of the spatial distribution of photofragments. The scheme is based on the orientational dependence of wave packet dynamics driven by an infrared laser pulse. Thus, the vibrational wave packets in the two hemispheres of a randomly oriented molecule are out of phase. Depending on the frequency of the ultraviolet control pulse, one can resonantly excite wave packets at a given position to a repulsive state. Since the wave packet position depends on the orientation, this implies that selective dissociation of one of two oppositely oriented molecules can be obtained. In order to obtain the desired selectivity, the ultraviolet control pulse must be shorter than one half of a vibrational period. In addition, a judicious balance between the spectral width (or, equivalently, the duration) of the ultraviolet pulse and the potential difference is required. Thus, if the pulse is too short, the selectivity will be lost.

The control scheme was applied to NaI. The full three-dimensional results show that with a proper timing of the control pulse, one particular fragment (e.g., only I atoms) will show up at the detector when it is positioned, say, in the forward direction with respect to the polarization axis of the pump laser. In addition, the angular distribution is strongly aligned $\propto\cos^4\theta$, due to the two independent excitations in the pump and the control step. We found very high selectivity for reasonable parameters of the pump and the control pulse.

Finally, some comments on the implications for the control scheme for selective bond breaking[3–5] described in the Introduction. In the computational studies presented previously, we studied symmetric triatomic (*ABA*) molecules with isotope substitutions. The infrared pump pulse excites, depending on the Hamiltonian, either a local bond mode or an antisymmetric stretch mode. We assumed a fixed orientation of the molecules with respect to the polarization of the laser field. Thus, the molecules have been *oriented* by an appropriate method prior to the application of the control scheme. The results of the present paper demonstrate clearly that the scheme can fail if the molecule is randomly oriented. Currently, we consider the extension of the scheme to molecules which initially are randomly oriented. To that end, we have demonstrated[12] how the orientation-dependent response of a molecule to a superposition of two infrared pump pulses can be used to obtain large oscillations for one orientation, while the vibrational amplitude for the opposite orientation remains small.

ACKNOWLEDGMENT

This work was supported by the Danish Natural Science Research Council.

APPENDIX: VIBRATIONAL EXCITATION IN A HARMONIC OSCILLATOR

We consider the interaction of a one-dimensional harmonic oscillator with a classical field within the electric dipole approximation for the interaction. The Hamiltonian takes the form

$$\hat{H}=-\frac{\hbar^2}{2M}\frac{\partial^2}{\partial q^2}+\frac{1}{2}M\omega_0^2q^2\pm\mu(R)E(t), \tag{A1}$$

where $q=(R-R_e)$. The minus sign in the last term describes the situation where the field and the dipole moment vector are pointing in the same direction, whereas the plus sign describes the situation where they have opposite directions. The electric dipole moment is expanded to first order around the equilibrium position R_e,

$$\mu(R)=\mu(R_e)+\mu'(R_e)q+\cdots, \tag{A2}$$

The Hamiltonian corresponds to a linearly forced harmonic oscillator.

The complete solution to the time-dependent Schrödinger equation can be expressed in terms of the solution for the corresponding classical equations of motion.[13] A complete set of solutions to time-dependent at most harmonic potentials is given by the generalized harmonic oscillator (GHO) states

$$\phi_n(q,t)=(2^n n!)^{-1/2}G(q,t)H_n[\kappa_t(q-q_t)]e^{-in\beta_t}, \tag{A3}$$

where $G(q,t)$ is a Gaussian wave packet

$$G(q,t)=\exp\left\{\frac{i}{\hbar}[\alpha_t(q-q_t)^2+p_t(q-q_t)+\gamma_t]\right\}, \tag{A4}$$

H_n is the nth Hermite polynomial, and

$$\kappa_t=(2\,\mathrm{Im}\,\alpha_t/\hbar)^{1/2},$$

$$\beta_t=\frac{2}{M}\int_0^t dt'\,\mathrm{Im}\,\alpha_{t'}. \tag{A5}$$

The q_t and p_t parameters are the expectation values of position and momentum

$$\langle\phi_n(t)|\hat{q}|\phi_n(t)\rangle=q_t,$$

$$\langle\phi_n(t)|\hat{p}|\phi_n(t)\rangle=p_t. \tag{A6}$$

In the following, we consider the dynamics of the GHO states with initial conditions corresponding to the stationary states of the free unforced oscillator. Thus, $q_0=p_0=0$ and $\alpha_0=iM\omega_0/2$. This choice for α_0 implies that $\alpha_t=\alpha_0$[13] and consequently that the uncertainties in position and momentum are time-independent. Thus, all the GHO states [including the Gaussian $\phi_0(q,t)=G(q,t)$]] are coherent states in the sense that the uncertainty is constant.

The time evolution of the expectation values of position and momentum is given by Hamiltons equations,

$$dq_t/dt=p_t/M, \tag{A7}$$

$$dp_t/dt = -M\omega_0^2 q_t \pm \mu'(R_e)E(t),$$

which implies that

$$d^2q_t/dt^2 + \omega_0^2 q_t = \pm\frac{\mu'(R_e)E(t)}{M}, \tag{A8}$$

and the initial values are $q_0 = p_0 = 0$. The solution can be written in the form

$$q_t = \pm\frac{\mu'(R_e)}{M\omega_0}\sin(\omega_0 t)\int_0^t E(t')\cos(\omega_0 t')dt' \mp\frac{\mu'(R_e)}{M\omega_0}\cos(\omega_0 t)\int_0^t E(t')\sin(\omega_0 t')dt'. \tag{A9}$$

Thus, q_t changes sign when the direction of the dipole moment vector $\boldsymbol{\mu}$ is reversed. In addition, we observe that for a superposition of fields, say $E(t) = E^{(1)}(t) + E^{(2)}(t)$, then $q_t = q_t^{(1)} + q_t^{(2)}$, i.e., a simple classical superposition corresponding to the effect of each field without interference terms.

For a rectangular pulse shape

$$E(t) = \begin{cases} 0 & t<0 \\ E_{\max}\cos(\omega t + \phi) & t>0, \end{cases} \tag{A10}$$

we get

$$q_t = \pm\frac{2A\omega_0}{\omega_0^2 - \omega^2}\{\cos(\omega t + \phi) + (\omega/\omega_0)\sin\phi\sin(\omega_0 t) - \cos\phi\cos(\omega_0 t)\}, \tag{A11}$$

where $A = \mu'(R_e)E_{\max}/(2\omega_0 M)$ and has the units of velocity. In the limit of a resonantly forced oscillator, $\omega \to \omega_0$, we obtain for $\phi = 0$

$$q_t = \pm At\sin(\omega_0 t), \qquad p_t = \pm AM\{\sin(\omega_0 t) + \omega_0 t\cos(\omega_0 t)\}. \tag{A12}$$

Thus, a simple forced motion. For $\phi = 3\pi/2$, the oscillator is driven by a pure sine field. In the resonant limit, we obtain

$$q_t = \pm A\{\sin(\omega_0 t)/\omega_0 - t\cos(\omega_0 t)\}, \qquad p_t = \pm AM\omega_0 t\sin(\omega_0 t). \tag{A13}$$

Thus, the phase of the field is important. The q_t oscillations are delayed with respect to the field by a phase factor $\pi/2$. The change of sign in Eq. (A9) for opposite orientation of field and dipole moment vector can be simulated by a change of the field phase by π.

Finally, we consider a field with a Gaussian pulse shape

$$E(t) = E_{\max}\exp\{-\alpha(t-t_c)^2\}\cos(\omega t), \tag{A14}$$

where $\alpha = (2\ln 2)/T_{\mathrm{FWHM}}^2$ and T_{FWHM} is the full width half maximum of the intensity pulse shape. The center of the pulse t_c is chosen such that $E(t) \sim 0$ for $t<0$. For $t \to \infty$, i.e., after the pulse is over, Eq. (A9) takes the form

$$q_t = \pm A(\pi/(2\ln 2))^{1/2}T_{\mathrm{FWHM}}[I_1\sin(\omega_0 t) - I_2\cos(\omega_0 t)], \tag{A15}$$

where

$$I_1 = \cos\{(\omega_0+\omega)t_c\}\exp\{-(\omega_0+\omega)^2/(4\alpha)\} + \cos\{(\omega_0-\omega)t_c\}\exp\{-(\omega_0-\omega)^2/(4\alpha)\},$$
$$I_2 = \sin\{(\omega_0+\omega)t_c\}\exp\{-(\omega_0+\omega)^2/(4\alpha)\} + \sin\{(\omega_0-\omega)t_c\}\exp\{-(\omega_0-\omega)^2/(4\alpha)\}. \tag{A16}$$

At resonance $\omega = \omega_0$ and in the limit of long pulses, $\omega_0^2 \gg \alpha$, we obtain

$$q_t = \pm A(\pi/(2\ln 2))^{1/2}T_{\mathrm{FWHM}}\sin(\omega_0 t). \tag{A17}$$

The result is now independent of t_c.

In the resonant case, the amplitude is proportional to the pulse area ($\propto E_{\max}T_{\mathrm{FWHM}}$) both for the rectangular and the Gaussian pulse shape. In the case of nonresonant forcing, the amplitude depends on A and a resonance criterion: $\omega_0/(\omega_0^2 - \omega^2)$.

[1] For reviews, see: R. J. Gordon and S. A. Rice, Annu. Rev. Phys. Chem. **48**, 601 (1997); *Chemical Reactions and Their Control on the Femtosecond Timescale*, Vol. 101 of *Advances in Chemical Physics*, edited by P. Gaspard and I. Burghardt (Wiley, New York, 1997); B. Kohler, J. L. Krause, F. Raksi, K. R. Wilson, and V. V. Yakovlev, Acc. Chem. Res. **28**, 133 (1995).

[2] M. J. Rosker, M. Dantos, and A. H. Zewail, J. Chem. Phys. **89**, 6113 (1988); for reviews see, e.g., *Femtosecond Chemistry*, Vols. I and II, edited by J. Manz and L. Wöste (VCH, Weinheim, 1995).

[3] B. Amstrup and N. E. Henriksen, J. Chem. Phys. **97**, 8285 (1992).

[4] B. Amstrup and N. E. Henriksen, J. Chem. Phys. **105**, 9115 (1996).

[5] M. Grønager and N. E. Henriksen, Chem. Phys. Lett. **278**, 166 (1997).

[6] R. B. Walker and R. K. Preston, J. Chem. Phys. **67**, 2017 (1977).

[7] E. Charron, A. Giusti-Suzor, and F. Mies, Phys. Rev. Lett. **75**, 2815 (1995); B. Sheehy, B. Walker, and L. F. DiMauro, *ibid.* **74**, 4799 (1995).

[8] H. L. Kim and R. Bersohn, J. Chem. Phys. **107**, 4546 (1997).

[9] S. Chelkowski, A. D. Bandrauk, and P. B. Corkum, Phys. Rev. Lett. **65**, 2355 (1990).

[10] E. Charron, A. Giusti-Suzor, and F. Mies, J. Chem. Phys. **103**, 7359 (1995).

[11] G. H. Peslherbe, R. Bianco, R. Hynes, and B. M. Ladanyi, J. Chem. Soc., Faraday Trans. **93**, 977 (1997).

[12] M. Machholm and N. E. Henriksen (unpublished).

[13] K. B. Møller and N. E. Henriksen, J. Chem. Phys. **105**, 5037 (1996).